UNIVERSITY OF BATH

Citation for published version:
Ye, J, Gao, B, Shepherd, P, Becque, J & Hajirasouliha, I 2017, 'A grid generation procedure for the design of single-layer freeform structures' Paper presented at IASS Annual Symposium 2017, Hamburg, Germany, 25/09/17 - 27/09/17, .

Publication date:
2017

Document Version
Publisher's PDF, also known as Version of record

Link to publication

University of Bath

A grid generation procedure for the design of single-layer free-form structures

Jun YE[a,b], Boqing GAO[b], Paul SHEPHERD[a], Jurgen BECQUE[c], Iman HAJIRASOULIHA[c],

*Department of Architecture and Civil Engineering, University of Bath
Bath, UK, BA2 7AY
Email: j.ye@bath.ac.uk
[a] Department of Architecture and Civil Engineering, University of Bath
[b] College of Civil Engineering and Architecture, Zhejiang University
[c] Department of Civil and Structural Engineering, University of Sheffield

Abstract

Computer aided design software enables the rapid creation of any curved surface geometry, whereas it is neither a convenient nor an obvious task for engineers to efficiently create a discrete grid structure on a complex surface that also meets architectural requirements. This emphasizes the importance of grid generating tools and methods in the initial design stage. This paper presents an efficient design tool for the synthesis of free-form grid structures based on the concept of a "guide line". The process starts with defining a limited number of curves (named the "guide lines") on the surface, which are then used to determine the directions of the 'rods' of the grid. Two variations of this concept are introduced in the paper: the 'Guide Line Scaling Method' (GSM) and the 'Two Guide Lines with Two End Vertices Method' (2G2VM). Case studies on the British Museum Court Roof are provided which illustrate the successful execution of these procedures. The results show that the free-form grid structures generated with the proposed methods feature a regular shape and fluent lines, thereby satisfying aesthetic requirements. These two methods have been programmed into the software ZD-Mesher, enabling rapid grid generation for structural design purposes.

Keywords: free-form surface, grid structure, guide line, free form structures, guide line scaling method.

1. Introduction

New techniques in computer aided design, such as parametric modelling and scripting, have enabled a new level of sophistication in design procedures. Among other developments, this has facilitated the increased inclusion of 3D free-form surfaces in structures, marrying the expression of architectural creativity with the application of cutting-edge technology. Complex free-form structures are one of the most visually striking trends in contemporary architecture. A number of structures with attractive designs and eye-catching shapes have recently been erected, as shown in Figures 1 (a) and (b). While they are constructed with sometimes vastly different materials, they all exemplify the emergence of free-form grid structures.

(a) British Museum Great Court (London, UK) (b) Toledo timber grid shell (Naples, Italy)[1]
Figure 1: Examples of free-form grid structures

If a curved surface with a suitable form is chosen and well-positioned supports are added, an efficient flow of the forces within the structure can be obtained [2], where a single layer grid-shell structure

consisting of a lattice of rods can be used to transmit the external loads down to the foundations by means of forces/bending moment within the members. This structural form often brings benefits in the form of reductions in material usage and an increase in unobstructed service space. However, it is not always obvious how to create an efficient grid structure on a given surface. Given the increasing popularity of free-form grid structures, a practical grid generation tool which can quickly and efficiently generate a structural grid on a given free-form surface is necessary in order to assist structural designers, particularly in the early design stage.

However, previous research on grid generating methodologies is rather limited. In general, topology optimization methods can be used to create an efficient structural grid on a predefined surface, as demonstrated by Park et al. [3] and Shepherd and Pearson [4]. Both studies presented an efficient layout optimization algorithm in order to generate grids for both single layer shells and double layer shells in the conceptual design stage. Wu et al. [5] conducted theoretical and experimental research on grid generation for a cable supported dome using topology optimization techniques. However, a drawback of all these topology optimization studies [3-5] is that the resulting topology is rather course and cannot directly be used in design (i.e. some refinement is required).

It seems that before the appearance of a design optimization tool that can provide optimum and practical solutions considering structural performance, it is sometimes more important to generate an aesthetically pleasing grid on a curved surface that satisfies the uniformity criteria, i.e. where unit cells have regular shapes and rods are composed of fluent lines. Therefore, most of the previous research studies have concentrated on mesh generation over a surface without taking into account structural performance. For example, Shepherd and Richens [2] proposed the Subdivision Surface method, where an initial triangular or quadrilateral mesh is first imposed onto a free-form surface and then subdivided over a number of iterations to fit the original surface.

This paper aims to develop a practical methodology to quickly generate a grid on a predefined curved surface with given boundaries, as a potential choice before taking into account of the optimum structural performance. It allows grid generation based on a limited number of guidelines using operations such as offset, scaling, rotation and projection. The methodology is innovative on the basis of introducing the concept of a "guideline" and two new ways of grid generation are presented, namely the 'guide line scaling' method (GSM) and the 'two guide lines with two end vertices' method (2G2VM). The algorithms have been implemented in the general-purpose programming language C++ and a Graphical User Interface was developed. A number of case studies are presented to illustrate the successful execution of the algorithms and the effectiveness of the software.

2. Guide line definition

To be practically relevant, the generated grid should meet certain aesthetic and architectural requirements. For a given surface there are various solutions which may satisfy those requirements, even when expressed in terms of objective criteria such as grid regularity, rod uniformity and pattern fluency. A simple example is shown in Figures 2 (b) and (c), where two grid patterns are considered: an orthogonal grid parallel to the sides and an orthogonal-diagonal grid. Which one is the more favourable pattern in terms of appearance most likely depends on the individual preference of the architect, although one could argue that the grid style presented in Figure 2 (c) portrays a sense of vividness and is therefore preferable.
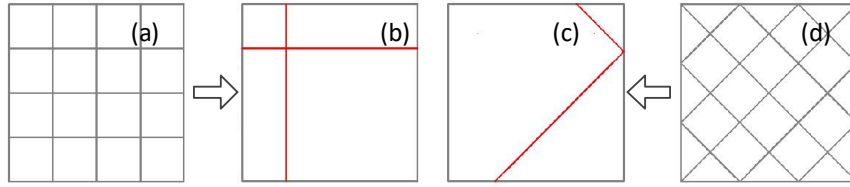
Figure 2: Guide lines and generated grid on a plane surface: (a) Guideline parallel to the edges; (b) Regular grid; (c) Diagonal grid at $45°$; (d) corresponding diagonal guide lines.

Given this context, a practical and feasible approach consists of defining a 'guide line' on the surface that sets the tone of the grid and reveals the intent of the designer. The red curves shown in Figure 2 (a) and Figure 2 (d) fulfill exactly this function in this simplified example.

3. Surface representation

In the proposed approach, the Non-Uniform Rational B-Spline (NURBS) is applied to describe curves and surfaces. To this end, the B-spline basis functions need to be introduced first. Let $\mathbf{U} = \{u_0, ..., u_n\}$ be a non-decreasing sequence of rational numbers, i.e., $u_i \leq u_{i+1}$, $i = 0, ..., n-1$. The numbers u_i are called the 'knots', and $\mathbf{U}$ is the 'knot vector'. The ith B-spline basis function of degree p, denoted by $N_{i,p}(u)$, is then defined in terms of an independent variable u as follows [6]:

$$N_{i,0}(u) = \begin{cases} 1 & \text{if } u_i \leq u < u_{i+1} \\ 0 & \text{otherwise} \end{cases}$$

$$N_{i,p}(u) = \frac{u - u_i}{u_{i+p} - u_i} N_{i,p-1}(u) + \frac{u_{i+p+1} - u}{u_{i+p+1} - u_{i+1}} N_{i+1,p-1}(u) \tag{1}$$

In the above equations, $i = 0, ..., n-p-1$, so that there are *n-p* basis functions of degree *p*. Note that $N_{i,0}(u)$ is a step function which is identically equal to zero everywhere, except in the half-open interval $u \in [u_i, u_{i+1})$. The higher order basis functions $N_{i,p}(u)$ are then formed by taking a linear combination of two basis functions of degree (*p*-1). The half-open interval $[u_i, u_{i+1})$ is commonly called the ith knot span. It can have zero length, since knots don't need to be distinct.

A pth-degree NURBS curve is defined by [6]:

$$\mathbf{C}(u) = \left(x(u), y(u), z(u)\right) = \frac{\sum_{i=0}^{n} N_{i,p}(u) w_i \mathbf{P}_i}{\sum_{i=0}^{n} N_{i,p}(u) w_i} \quad a \leq u \leq b \tag{2}$$

where $\mathbf{P}_i = (x_i, y_i, z_i)$ are the control points, w_i are the weight factors, n is the number of control points and $N_{i,p}(u)$ are the pth-degree B-spline basis functions according to Eq. (1), defined on the knot vector:

$$\mathbf{U} = \{\underbrace{a, ..., a}_{p+1}, u_{p+1}, ..., u_{r-p-1}, \underbrace{b, ..., b}_{p+1}\} \tag{3}$$

where $r = n + p + 1$ is the number of knots. Adding the zero length knot spans in Eq. (3) ensures that there are exactly $n + 1$ basis functions of degree p. It is also noted that w_i are restrained to positive values for all i values. Introducing the notation:

$$R_{i,p}(u) = \frac{N_{i,p}(u)w_i}{\sum_{j=0}^{n} N_{j,p}(u)w_j}$$ (4)

Eq. (2) can be rewritten in the form:

$$\mathbf{C}(u) = \sum_{i=0}^{n} R_{i,p}(u) \cdot \mathbf{P}_i$$ (5)

where $\{R_{i,p}(u)\}$ are the rational basis functions, which are also piecewise rational functions of $u \in [a,b]$.

In general, NURBS defined curves have the following two important geometric characteristics [6, 7], which will prove useful at a later stage:

(1) $\sum_{i=0}^{n} R_{i,p}(u) = 1$ for all $u \in [a,b]$, which, together with $R_{0,p}(a) = R_{n,p}(b) = 1$, implies: $\mathbf{C}(a) = \mathbf{P}_0$ and $\mathbf{C}(b) = \mathbf{P}_n$. In other words, the starting point of the curve is the first control point, while the end point of the curve is the last control point.

(2) Affine invariance: an affine transformation can be applied to the curve by applying it to the control points. Affine transformations include translations, rotations, scaling and shearing. NURBS curves are also invariant under perspective projections.

A NURBS surface of degree p in the u direction and degree q in the v direction is a bivariate vector-valued piecewise rational function of the form [6]:

$$\mathbf{S}(u,v) = \frac{\sum_{i=0}^{n}\sum_{j=0}^{m} N_{i,p}(u)N_{j,q}(v)w_{i,j}\mathbf{P}_{i,j}}{\sum_{i=0}^{n}\sum_{j=0}^{m} N_{i,p}(u)N_{j,q}(v)w_{i,j}} \quad a \leq u \leq b, c \leq v \leq d$$ (6)

where $\mathbf{P}_{i,j}$ forms a bidirectional control net of points, $w_{i,j}$ are the weight factors and $N_{i,p}(u)$ and $N_{j,q}(v)$ are the non-uniform rational B-spline basis functions defined on the knot vectors:

$$\begin{cases} \mathbf{U} = \{\underbrace{a,...,a}_{p+1},u_{p+1},...,u_{r-p-1},\underbrace{b,...,b}_{p+1}\} \\ \mathbf{V} = \{\underbrace{c,...,c}_{q+1},v_{q+1},...,v_{s-q-1},\underbrace{d,...,d}_{q+1}\} \end{cases}$$ (7)

where $r = n + p + 1$ and $s = m + q + 1$.

The above NURBS equations defining a surface and a curve can be used to represent the curved architectural surface and the guideline for grid generation discussed in the previous sections. It is thereby noted that, since the guideline necessarily lies on the surface, the guideline also has a 2D

representation in the parameter space (u,v) of the surface. Let (u,v) be the definitional domain of the surface $\mathbf{S}(u,v)$. The 3D guideline on the surface $\mathbf{S}(u,v)$ can then be seen as the result of a two-time mapping procedure, where the pair (u,v) is first calculated from the parameter w using a function $\mathbf{C}(w)$. The value domain of the curve $\mathbf{C}(w)$ is thus part of the definitional domain of the surface $\mathbf{S}(u,v)$. The three-dimensional coordinates of the guide line are then calculated from the pair of parameters (u,v) using the surface function $\mathbf{S}(u,v)$. It is obvious that all of the coordinates obtained by this two-time mapping method lie exactly on the surface, so that the guide line is embedded within the curved surface.

A three-dimensional curve can easily be obtained from its two-dimensional representation by the above mapping procedure. The solution to the inverse problem (obtaining the 2D representation when the curve is known in 3D space) is documented in [6].

4. Guide line scaling method (GSM)

In the GSM, the following steps are taken (Fig. 3):

1. An initial guide line is sketched on the curved surface. Alternatively, one of the boundaries of the surface may in some cases be selected as a guide line.

2. A NURBS representation $\mathbf{S}(u,v)$ is fitted to the surface, while the initial guide line defined on the surface in Step 1 is represented by an NURBS curve $\mathbf{C}_0$ in three-dimensional space. The control points of the NURBS curve $\mathbf{C}_0$ are $\mathbf{P}_i$, $i = 0,1,...,n$. $\mathbf{P}_0$ and $\mathbf{P}_n$ are the first and the last control points, which are also the two end points of the curve (as explained in Section 3).
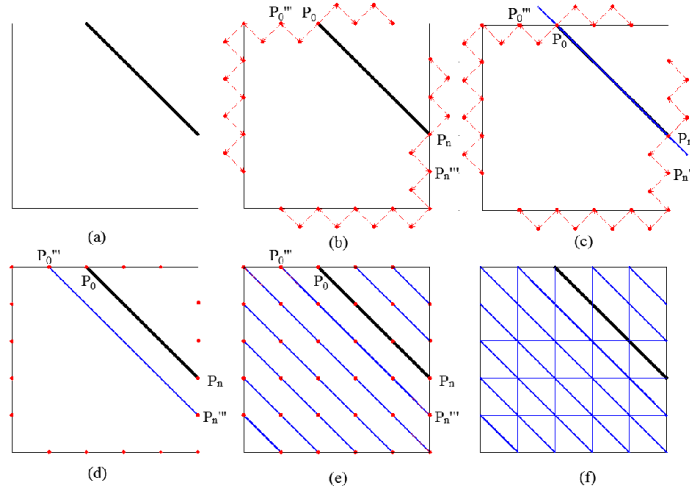

Figure 3: Main steps of GSM, as schematically illustrated for a flat surface: (a) definition of initial guide line; (b) generation of new end points; (c) scaling of the guideline; (d) translation/rotation of the guideline, followed by projection onto the surface; (e) generation of grid points; (f) final triangular grid

3. In order to generate a new curve on the surface in the shape of the original guide line, the end points of the original guide line $\mathbf{P}_0$ and $\mathbf{P}_n$ are first moved forward in space by a constant (chosen) distance L in the direction of the vector $\bar{\mathbf{D}} = \pm\bar{\mathbf{N}} \times \bar{\boldsymbol{\tau}}$ (as shown in Figure 4). $\bar{\mathbf{N}}$ is the normal vector of the surface calculated at those respective points and $\bar{\tau}$ is the tangent vector of the guide line. Therefore, $\bar{\mathbf{D}}$ constitutes a direction perpendicular to the guide line in the tangent plane of the surface. It is clear that, in general, these new points do not lie on the surface boundary. Each point is therefore projected

down to the boundary by finding the intersection of a plane perpendicular to $\bar{\mathbf{D}}$ through the new point and the boundary. Let these two end points of the new curve, located on the boundary of the surface, be called $\mathbf{P}_0'''$ and $\mathbf{P}_n'''$.

4. $\mathbf{P}_0'''$ and $\mathbf{P}_n'''$ are then connected with a new curve in the shape of the original guideline. An affine transformation of the original guideline which, in the general case, consists of a scaling, a translation and a rotation, is thereby necessary.

Let l_1 be the Euclidean distance between $\mathbf{P}_0$ and $\mathbf{P}_n$, while the Euclidean distance between $\mathbf{P}_0'''$ and $\mathbf{P}_n'''$ is denoted by l_2. If $l_1 \neq l_2$, a scaling of the original guide line is required:

$$\mathbf{P}_i' = (\mathbf{P}_i - \mathbf{P}_n) \times l_2 \div l_1 + \mathbf{P}_n , \ i = 0,1,...,n \tag{8}$$

where $\mathbf{P}_i'$ are the control points of the scaled curve.

The control points are then translated according to the formula below:

$$\mathbf{P}_i'' = \mathbf{P}_i' + (\mathbf{P}_n''' - \mathbf{P}_n), \ i = 0,1,...,n \tag{9}$$

where $\mathbf{P}_i''$ are the control points after the curve is scaled and translated.
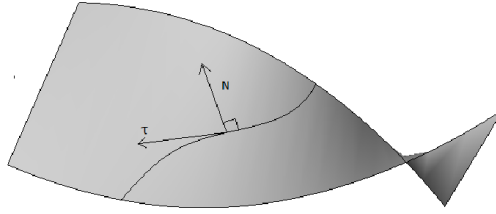

Figure 4: Advancing direction of the guide line

If $\mathbf{P}_0''$ and $\mathbf{P}_0'''$ happen to coincide with each other, then the translated control points are the end points of the new curve. In general, however, $\mathbf{P}_0''$ and $\mathbf{P}_0'''$ do not coincide and the scaled and translated guideline also needs to be rotated so that $\mathbf{P}_0''$ and $\mathbf{P}_0'''$ coincide, as shown in Figure 5.

(a) $\mathbf{P}_0''$ and $\mathbf{P}_0'''$ are coinciding   (b) $\mathbf{P}_0''$ and $\mathbf{P}_0'''$ are not coinciding
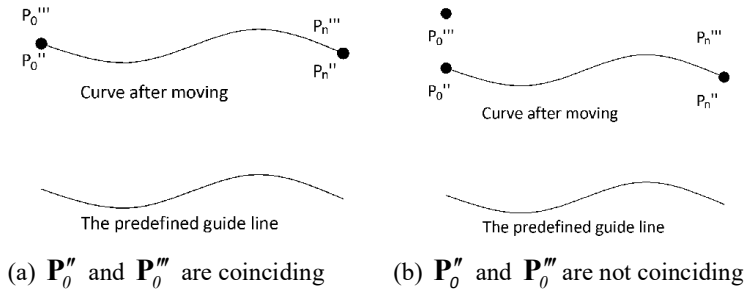
Figure 5: Adjustment of the generated curves

The axis of rotation $\mathbf{R}$ is the line through point $\mathbf{P}_n'' (= \mathbf{P}_n''')$ perpendicular to the plane determined by the three points: $\mathbf{P}_0'''$, $\mathbf{P}_0''$ and $\mathbf{P}_n''$:

$$\mathbf{R} = (\mathbf{P}_0'' - \mathbf{P}_n'') \times (\mathbf{P}_0''' - \mathbf{P}_n'') \tag{10}$$

The angle of rotation γ is determined by:

$$\gamma = 2\arcsin \frac{\left| \mathbf{P}_0''' - \mathbf{P}_0'' \right|}{2\left| \mathbf{P}_0'' - \mathbf{P}_n'' \right|} \tag{11}$$

The coordinates of the new control points $\mathbf{P}_i'''$ can then be obtained from the coordinates of $\mathbf{P}_i''$ through a coordinate transformation. A new curve is subsequently defined by the control points $\mathbf{P}_i'''$ and the same weight factors, knot vector and degree as the original guide line. However, this curve $\mathbf{C}_I$, in the general case, does not lie on the original curved surface $\mathbf{S}(u,v)$.

5. A number of discrete points on the curve $\mathbf{C}_I$ are projected perpendicularly onto the surface $\mathbf{S}(u,v)$. In order to achieve this for a generic point $\mathbf{P} = (x, y, z)$, the following vector field is first defined:

$$\mathbf{r}(u,v) = \mathbf{S}(u,v) - \mathbf{P} \tag{12}$$

which is made subject to the following two conditions:

$$\begin{cases} \mathbf{f}(u,v) = \mathbf{r}(u,v) \cdot \mathbf{S}_u(u,v) = 0 \\ \mathbf{g}(u,v) = \mathbf{r}(u,v) \cdot \mathbf{S}_v(u,v) = 0 \end{cases} \tag{13}$$

The above equations express that a point on the surface $\mathbf{S}(u,v)$ needs to be found at which the normal to the surface points to the point $\mathbf{P} = (x, y, z)$. The above equations can be solved iteratively by defining the following matrices in the ith iteration:

$$\boldsymbol{\delta}_i = \begin{bmatrix} \Delta u \\ \Delta v \end{bmatrix} = \begin{bmatrix} u_{i+1} - u_i \\ v_{i+1} - v_i \end{bmatrix} \tag{14}$$

$$\mathbf{J}_i = \begin{bmatrix} \mathbf{f}_u & \mathbf{f}_v \\ \mathbf{g}_u & \mathbf{g}_v \end{bmatrix} = \begin{bmatrix} \left| \mathbf{S}_u \right|^2 + \mathbf{r} \cdot \mathbf{S}_{uu} & \mathbf{S}_u \cdot \mathbf{S}_v + \mathbf{r} \cdot \mathbf{S}_{uv} \\ \mathbf{S}_u \cdot \mathbf{S}_v + \mathbf{r} \cdot \mathbf{S}_{vu} & \left| \mathbf{S}_v \right|^2 + \mathbf{r} \cdot \mathbf{S}_{vv} \end{bmatrix} \tag{15}$$

$$\boldsymbol{\kappa}_i = -\begin{bmatrix} \mathbf{f}(u_i, v_i) \\ \mathbf{g}(u_i, v_i) \end{bmatrix} \tag{16}$$

All the functions in the matrix $\mathbf{J}_i$ are thereby evaluated at the point (u_i, v_i). In the ith iteration, the 2×2 system of linear equations in the unknown $\boldsymbol{\delta}_i$ is solved:

$$\mathbf{J}_i \boldsymbol{\delta}_i = \boldsymbol{\kappa}_i \tag{17}$$

After obtaining $\boldsymbol{\delta}_i$ the new coordinates are calculated:

$$u_{i+1} = u_i + \Delta u, \quad v_{i+1} = v_i + \Delta v \tag{18}$$

The convergence criteria are thereby given by:

$$\left| \mathbf{S}(u_i, v_i) - \mathbf{P} \right| \le \varepsilon_1 \tag{19}$$

$$\frac{\left|\mathbf{S}_u(u_i,v_i)\cdot(\mathbf{S}(u_i,v_i)-\mathbf{P})\right|}{\left|\mathbf{S}_u(u_i,v_i)\right|\left|\mathbf{S}(u_i,v_i)-\mathbf{P}\right|}\le\varepsilon_2,\quad\frac{\left|\mathbf{S}_v(u_i,v_i)\cdot(\mathbf{S}(u_i,v_i)-\mathbf{P})\right|}{\left|\mathbf{S}_v(u_i,v_i)\right|\left|\mathbf{S}(u_i,v_i)-\mathbf{P}\right|}\le\varepsilon_2 \qquad (20)$$

At the same time, it should be checked in each iteration whether the points (u_i,v_i) remain within the boundaries of the surface $\mathbf{S}(u,v)$.

6. After the projected points on the surface $\mathbf{S}(u,v)$ are obtained, the corresponding points (u,v) in the parameter space are calculated. A 2D NURBS curve is then fitted through these points in the parameter space and mapped back onto the 3D surface. This is done to ensure that the new curve is completely embedded within the surface $\mathbf{S}(u,v)$.

7. The above procedure is then repeated a sufficient number of times by advancing successive curves to cover the whole surface. These curves are then subdivided along their lengths into an integer number of segments with equal chord length, approximately equal to the preferred rod length of the grid. Corresponding points on adjacent curves are then connected to form a triangular lattice.

5. Two guide lines with two end vertices method (2G2VM)
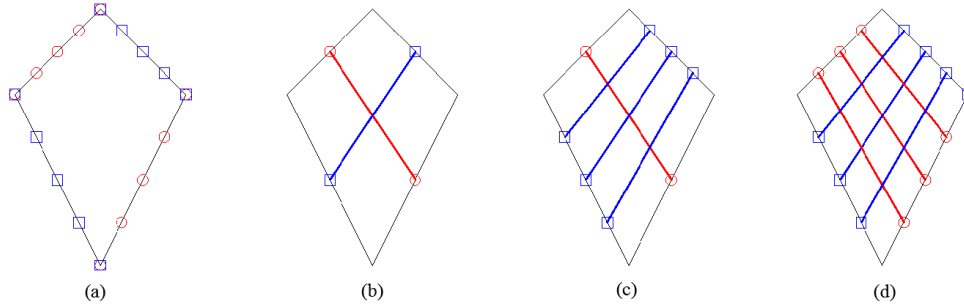

(a)   (b)   (c)   (d)

Figure 6: Main steps of the 2G2VM, shown schematically for a flat surface: (a,b) Two initial guide lines are defined and boundaries are divided; (c) New curves are generated by advancing the first guide line; (d) Second guide line is advanced to generate a grid.

In contrast with the GSM, the 2G2VM requires the definition of not one, but two initial guide lines. Each of the guide lines intersects at its ends with two of the surface boundaries. These boundaries are subsequently subdivided into a number of equal (chord) length intervals separated by 'vertices'. The original guide line is then advanced by moving the end points to the next two vertices on the boundaries while applying steps 4-6 of the previous section. The process is repeated for the remaining vertices. An identical procedure is then applied to the second guide line. The intersecting points of both sets of guide lines eventually form the nodes of the grid. The main steps of the 2G2VM are shown schematically for a pair of red and blue guide lines in Figure 6.

6. British Museum Great Court Roof

The steel and glass roof of the British Museum Great Court covers a rectangular area which is 70 m in width and 100 m in length. The Reading Room, which has a cylindrical shape with a diameter of 44 m, is located at the centre of the court. The shape of the roof can be expressed as a mathematical function and more information is provided in [8]. The rods in the roof range in length from 1 m to 3 m. As an additional case study the here proposed methods (GSM and 2G2VM) were applied to generate a grid on the roof of the British Museum Great Court. The original surface and mesh are shown in Figs. 7 (a) and (b), respectively.

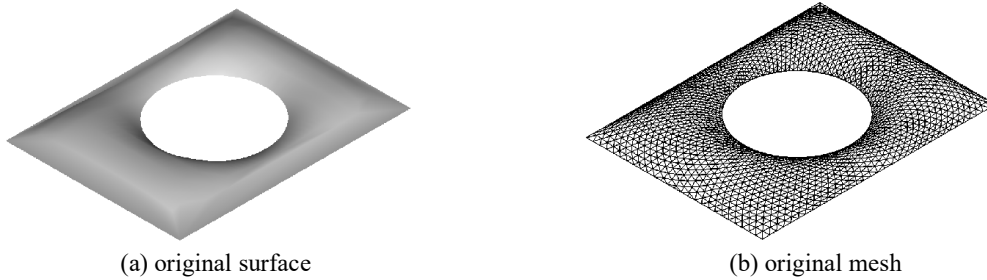(a) original surface   (b) original mesh

Figure 7: The British Museum Great Court roof

The surface was first divided into four sub-surfaces using the diagonals of the rectangular plan. Each method was then applied to the sub-surfaces, after which the grids of the sub-surfaces were merged together. Some of the intermediate steps, as well as the final grid resulting from the GSM are shown in Figs. 8. Figs. 9 illustrate the intermediate and final results using the 2G2VM.

The triangular grid pattern on the British Museum Great Court roof surface obtained using the GSM, pictured in Fig. 8(c), has somewhat similar features to the original design and shows very good fluency. However, the rod length is more uniform in the GSM grid, due to the fact that the algorithm was developed specifically with rod uniformity in mind. Fig. 9(c) illustrates the quadrilateral grid generated using the 2G2VM. The fluency of the pattern and the uniformity of the rods are both very good, although some irregular cells are encountered along the boundary lines of the sub-surfaces.

The mean value and the variance of the rod lengths were calculated for each of the three grid patterns and are compared in Table 1. While the mean values of the rod lengths are approximately the same, the variance of the rod lengths is reduced by 42% compared to the original grid when using the GSM. This again illustrates the advantage of the GSM in obtaining uniform grids. On the contrary, the quadrilateral grid generated using the 2G2VM is far less uniform than the original triangular grid.

Both proposed grid generation methodologies (GSM and 2G2VM) were programmed into software called 'ZD-Mesher', specifically developed by the authors for the purpose of free-form grid generation. The software was developed for a Microsoft Windows operating system, using C++ and the IDE of Microsoft Visual Studio 2013. The GUI framework was based on MFC (Microsoft Foundation Classes.

(a) Advancing the guide line on   (b)Segmentation and   (c) Results
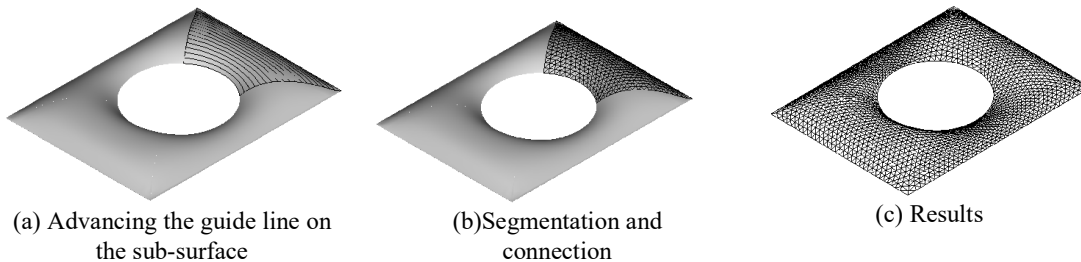   the sub-surface   connection

Figure 8: Steps of grid generation using the GSM on the British Museum Great Court roof

Table 1: Mean value and variance of the rod lengths in three grids

Grid generation method	Mean value of rod lengths (mm)	Variance of rod lengths (mm^2)
Original Mesh (triangular)	2047	207150
GSM (triangular)	2032	120136
2G2VM (diamond)	2126	464820

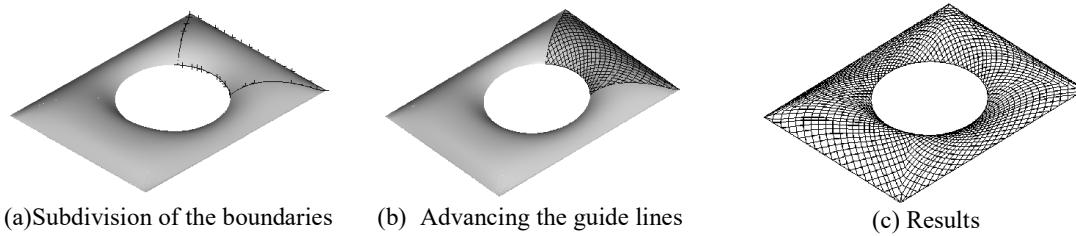(a) Subdivision of the boundaries   (b) Advancing the guide lines   (c) Results

Figure 9: Steps of grid generation using the 2G2VM on the British Museum Great Court roof.

7. Conclusions

The paper presents an efficient design tool for grid generation on a free-form surface. The proposed methods are based on the concept of a guide line, which allows an initial expression of architectural intent. The guide line is advanced over the surface by moving the endpoints, performing an affine transformation of the guide line and projecting it back onto the surface. Two variations are presented: the GSM, where a single guide line is used and the resulting curves are broken into segments, and the 2G2VM, where the grid is obtained as the intersection points of two sets of curves, each obtained by advancing a guide line. Both methods draw on the use of NURBS to mathematically represent surfaces and curves. Some practical case studies for both the GSM and 2G2VM are provided. The results indicate that a diverse range of constructible and visually expressive solutions can be obtained

Acknowledgements

References

[1] D'Amico B., Kermani A. and Zhang H., Form finding and structural analysis of actively bent timber grid shells. *Engineering Structures*, 2014; **81**; 195-207.

[2] Shepherd P. and Richens P., The case for subdivision surfaces in building design, *Journal of the International Association for Shell and Spatial Structures*, 2012; **53**; 237-245.

[3] Park P., Gilbert M., Tyas A. and Popovic-Larsen O., Potential use of structural layout optimization at the conceptual design stage. *International Journal of Architectural Computing*, 2012; **10**; 13-32.

[4] Shepherd P. and Pearson W., Topology optimisation of algorithmically generated space frames, in IASS 2013. *Beyond the Limit of Man*, Poland, 2013.

[5] Wu H., Ye J., Gao B.Q., Shan Y.L. and Zhang C., On the robustness of cable supported structures, a theoretical and experimental study. *Journal of the International Association for Shell and Spatial Structures*, 2014; **55**; 243-56.

[6] Piegl L. and Tiller W., *The NURBS book*, Springer Science & Business Media, 2012.

[7] Piegl L., On NURBS: a survey. *IEEE Computer Graphics and Applications*, 1991; 55-71.

[8] Williams CJ. The analytic and numerical definition of the geometry of the British Museum Great Court Roof, in Mathematics & design 2001, Deakin University, 2001, 434-440.